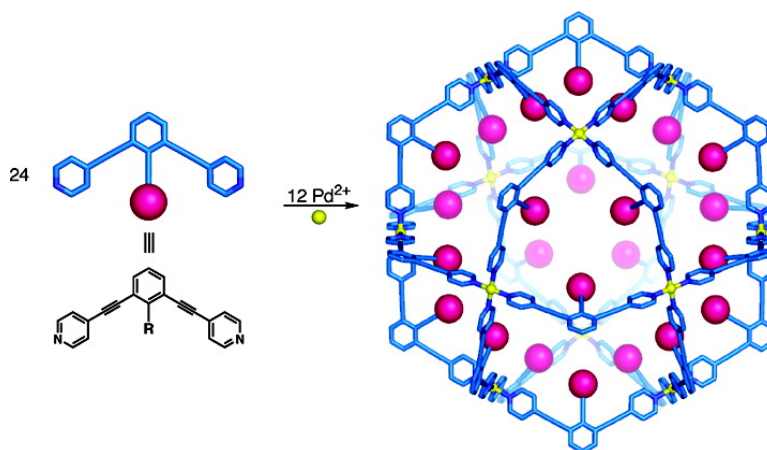


24-Fold Endohedral Functionalization of a Self-Assembled ML Coordination Nanoball

Masahide Tominaga, Kosuke Suzuki, Takashi Murase, and Makoto Fujita

J. Am. Chem. Soc., **2005**, 127 (34), 11950-11951 • DOI: 10.1021/ja054069o • Publication Date (Web): 09 August 2005

Downloaded from <http://pubs.acs.org> on March 25, 2009



More About This Article

Additional resources and features associated with this article are available within the HTML version:

- Supporting Information
- Links to the 27 articles that cite this article, as of the time of this article download
- Access to high resolution figures
- Links to articles and content related to this article
- Copyright permission to reproduce figures and/or text from this article

[View the Full Text HTML](#)

24-Fold Endohedral Functionalization of a Self-Assembled $M_{12}L_{24}$ Coordination Nanoball

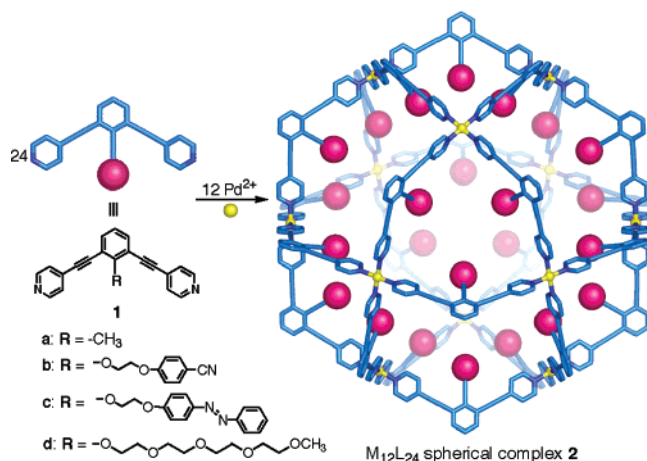
Masahide Tominaga, Kosuke Suzuki, Takashi Murase, and Makoto Fujita*

Department of Applied Chemistry, School of Engineering, The University of Tokyo, CREST, Japan Science and Technology Corporation (JST), 7-3-1 Hongo, Bunkyo-ku, Tokyo 113-8656, Japan

Received June 20, 2005; E-mail: mfujita@appchem.t.u-tokyo.ac.jp

Biological giant hollow structures, such as a family of spherical viruses, have highly functionalized shell interior for efficient interaction with substances (e.g., DNA) which are stored within the shells.¹ Contrary to this, the voids of artificial hollow compounds are, in general, too small to be functionalized.² Endohedral functionalization is limited only to polymer materials, such as mesoporous silica gel³ or micelles,⁴ which do not have well-defined structures and shapes. Here, we report the 24-fold endohedral functionalization of a large hollow coordination cage. The shell of the cage consists of 12 metals and 24 ligands and has a roughly spherical shape with the symmetry of cuboctahedron.^{5,6} Each ligand has a bis(4-pyridyl)-substituted bent framework involving two acetylene spacers. When complexed with Pd^{2+} ions, the ligand assembles quantitatively into the $M_{12}L_{24}$ spherical complex. We show that, by putting a functional group at the curvature of the bent ligand, the 24 functional groups are precisely arrayed inward within the spherical complex (Scheme 1).

Scheme 1. Self-Assembly of $M_{12}L_{24}$ Complexes with 24 Endohedral Functional Groups



To align 24 functional groups at the interior surface of the spherical complex, we prepared ligand **1a** by the Sonogashira cross-coupling reaction⁷ of 4-ethynylpyridine with 2,6-dibromotoluene. When ligand **1a** (0.02 mmol) was treated with $Pd(NO_3)_2$ (0.01 mmol) in $DMSO-d_6$ (1 mL) for 4 h at 70 °C, the formation of a single product was indicated by 1H NMR spectroscopic analysis (Figure 1). The five proton signals (H_{a-e}) agree with the formation of spherical complex **2a**. The large downfield shifts of the protons of pyridine rings (e.g., $\Delta\delta_{Py\alpha} = 0.59$ ppm) can be ascribed to the metal–ligand complexation. After anion exchange from NO_3^- to OTf^- , cold-spray ionization mass spectroscopy (CSI-MS)⁸ clearly confirmed an $M_{12}L_{24}$ composition with the molecular weight of 11919 Da as evident from prominent peaks of $[2a-(OTf^-)_m + (DMSO)_n]^{m+}$ ($m = 6-16$, $n = 0-12$). For example, in the 12^+

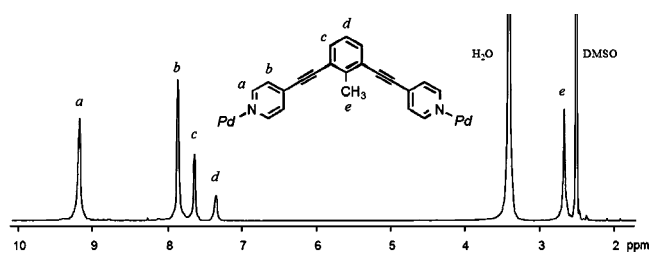


Figure 1. 1H NMR spectrum of **2a** (500 MHz, $DMSO-d_6$, 300 K, TMS).

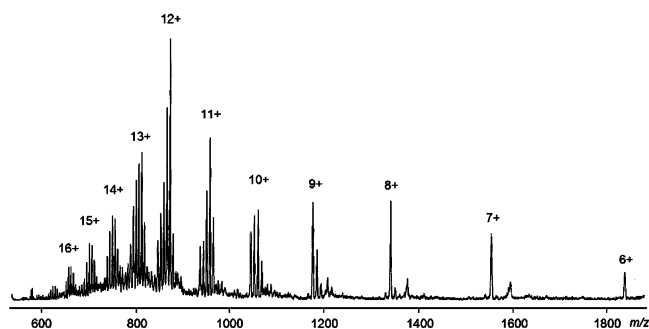
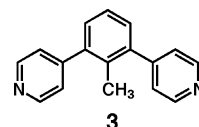


Figure 2. CSI-MS spectrum of **2a** ($CH_3CN:DMSO = 20:1$, OTf^- salt).

region, the peak at m/z 870.1 was assigned to $[2a-(OTf^-)_{12} + (DMSO)_4]^{12+}$ (Figure 2). A clear AFM image was observed for **2b** (Figure 3), strongly supporting the formation of a 4–5 nm-sized molecular particle and revealing the stability of the complex under AFM conditions.

In the endohedral functionalization of the $M_{12}L_{24}$ sphere, the acetylene spacer of the ligand plays two important roles. First, the acetylene spacer expands the cavity of the complex. The diameter and the longest Pd–Pd distance of the sphere are 4.6 and 3.5 nm, respectively, being considerably larger than those of the spherical complex without the acetylene spacer.⁵ Second, the acetylene spacer prevents the ligand from taking unfavorable nonplanar conformation, which is caused by steric repulsion between the pyridyl groups and the core benzene ring when the acetylene spacer is absent. For example, ligand **3** having no acetylene spacer adopts twisted conformation and does not assemble into the $M_{12}L_{24}$ complex upon complexation with Pd(II) ions. At each Pd(II) center of the $M_{12}L_{24}$ complex, a perpendicular array of four pyridyl groups with respect to the PdN_4 plane seems to be essential to the self-assembly of the spherical complex.



Thanks to the extraordinarily large cavity of the molecular sphere, a variety of functional groups can be appended at the interior

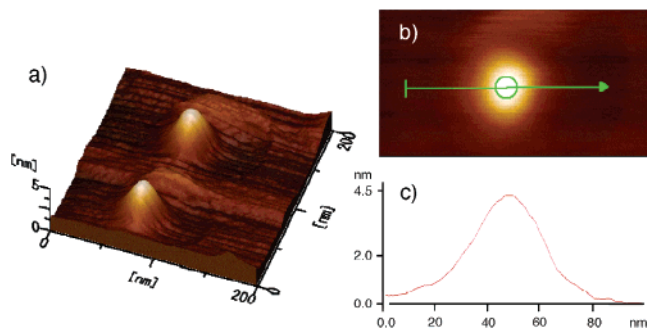


Figure 3. AFM image of **2b** on mica: (a) 3D image; (b) 2D image; and (c) its height profile.

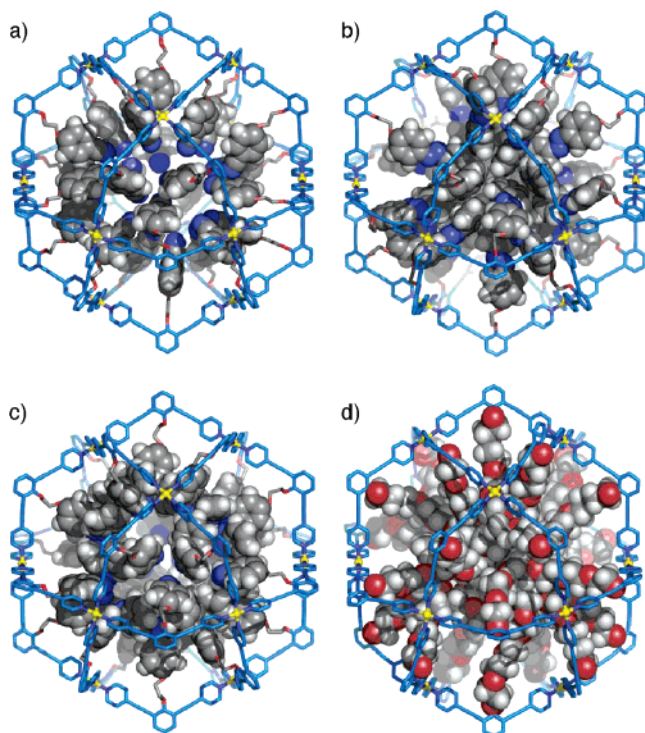


Figure 4. Molecular modeling of (a) **2b**, (b) **2c** (trans form), (c) **2c** (cis form), and (d) **2d** optimized by a force-field calculation with Cerius² 3.5.

surface. Ligand **1b** with a cyanophenyl appendix was assembled into $M_{12}L_{24}$ sphere **2b** upon complexation with Pd(II). At the core of **2b**, 24 cyano groups were highly concentrated (Figure 4a), potentially making possible the insulation of metal or metal oxide clusters therein via cyano coordination. Sphere **2c**, assembled from **1c** and Pd(II), included 24 photoresponsive azobenzene units (Figure 4b). A modeling study predicted considerable free volume change of the cavity upon trans–cis isomerization (Figure 4c). Ligand **1d** with an oligo(ethylene oxide) chain was assembled into sphere **2d**, whose cavity was filled with a “pseudo-nanoparticle” of poly(ethylene oxide) (Figure 4d). This pseudo-nanoparticle, containing 120 ether oxygen atoms, has a well-defined structure with a spherical shape (4.6 nm in diameter) and no size and molecular weight distributions. The structures of **2b–2d** were reliably characterized by ¹H NMR and CIS-MS (Supporting Information).⁹

Particularly interesting is that the poly(ethylene oxide) pseudo-nanoparticle insulated within spherical complex **2d** absorbed metal ions quite efficiently. When complex **2d** was mixed with rare earth metal ions and alkaline earth metal ions, ¹H NMR spectroscopic studies indicated the formation of metal–ethyleneoxide complex inside **2d**. For example, when **2d** (0.83 mM) was mixed with La(OTf)₃ (12 molar equiv) in CD₃CN, outstanding downfield shifts

were observed for the signal of $-CH_3$ ($\Delta\delta = 0.13$ ppm). In contrast, the signals of the shell of **2d** remained almost unchanged. These results indicated the selective binding of La(III) ions at the ether oxygen atoms of the pseudo poly(ethylene oxide) core. The complexation ratio of La(III) ion to each (OCH₂CH₂)₄OMe chain was estimated to be roughly 1:1 by the Job’s plot (Supporting Information). This indicated that the sphere contained ca. 20 La(III) ions within the shell. Interestingly, the absorbed metal ions were expelled by adding a coordinative solvent, such as DMSO. Thus, upon the addition of DMSO (5 vol %), the broad signals of the ethylene oxide chain were sharpened and the chemical shifts of these protons became identical to that of La(III)-free **2d** in 5 vol % DMSO/CD₃CN.

In summary, we have demonstrated the 24-fold functionalization at the interior surface of a spherical complex. The facile endohedral multi-functionalization is mainly indebted to two factors. The first is the extraordinarily large cavity of the $M_{12}L_{24}$ spherical complex that can accommodate 24 functional groups. The second is the spontaneous and quantitative self-assembly of the spherical shell from 36 components. By utilizing such a unique method for “endohedral molecular coating”, well-defined nanospace surrounded by various types of the interior surfaces can be provided at will, as currently investigated in our laboratory.

Supporting Information Available: Preparation and physical properties of **1a–1d**, **2a–2d**, and Job’s plot of **2d** and La(III) ions. This material is available free of charge via the Internet at <http://pubs.acs.org>.

References

- (1) (a) Speir, J. A.; Munshi, S.; Wang, G.; Baker, T. S.; Johnson, J. E. *Structure* **1995**, *3*, 63–78. (b) Douglas, T.; Young, M. *Nature* **1998**, *393*, 152–155. (c) Reinisch, K. M.; Nibert, M. L.; Harrison, S. C. *Nature* **2000**, *404*, 960–967. (d) Lucas, R. W.; Larson, S. B.; McPherson, A. J. *Mol. Biol.* **2002**, *317*, 95–108. (e) Dragnea, B.; Chen, C.; Kwak, E.-S.; Stein, B.; Kao, C. C. *J. Am. Chem. Soc.* **2003**, *125*, 6374–6375.
- (2) (a) Boxter, P.; Lehn, J.-M.; DeCian, A.; Fischer, J. *Angew. Chem., Int. Ed. Engl.* **1993**, *32*, 69–72. (b) Meissner, R. S.; Rebeck, J., Jr.; de Mendoza, J. *Science* **1995**, *270*, 1485–1488. (c) Fujita, M.; Oguro, D.; Miyazawa, M.; Oka, H.; Yamaguchi, K.; Ogura, K. *Nature* **1995**, *378*, 469–471. (d) Beissel, T.; Power, R. E.; Raymond, K. N. *Angew. Chem., Int. Ed. Engl.* **1996**, *35*, 1084–1086. (e) MacGillivray, L. R.; Atwood, J. L. *Nature* **1997**, *389*, 469–472. (f) Olenyuk, B.; Whiteford, J. A.; Fechtenkötter, A.; Stang, P. J. *Nature* **1999**, *398*, 796–799.
- (3) (a) Feng, X.; Fryxell, G. E.; Wang, L. Q.; Kim, A. Y.; Liu, J.; Kemner, K. M. *Science* **1997**, *276*, 923–926. (b) Lim, M. H.; Blanford, C. F.; Stein, A. J. *Am. Chem. Soc.* **1997**, *119*, 4090–4091. (c) Inagaki, S.; Guan, S.; Ohsumi, T.; Terasaki, O. *Nature* **2002**, *304*, 304–307. (d) Liu, N.; Chen, Z.; Dunphy, D. R.; Jiang, Y.-B.; Assink, R. A.; Brinker, C. J. *Angew. Chem., Int. Ed.* **2003**, *42*, 1731–1734. (e) Radu, D. R.; Lai, C.-Y.; Wiench, J. W.; Pruski, M.; Lin, V. S.-Y. *J. Am. Chem. Soc.* **2004**, *126*, 1640–1641.
- (4) (a) Oehme, G.; Paetzold, E.; Selke, R. *J. Mol. Catal.* **1992**, *71*, L1–L5. (b) Kataoka, K.; Togawa, H.; Harada, A.; Yasugi, K.; Matsumoto, T.; Katayose, S. *Macromolecules* **1996**, *29*, 8556–8557. (c) Brettreich, M.; Hirsch, A. *Tetrahedron Lett.* **1998**, *39*, 2731–2734. (d) Jin, R.-H. *Adv. Mater.* **2002**, *14*, 889–892. (e) Kang, Y.; Taton, T. A. *J. Am. Chem. Soc.* **2003**, *125*, 5650–5651. (f) Adams, M. L.; Lavasanifar, A.; Kwon, G. S. *J. Pharm. Sci.* **2003**, *92*, 1343–1355.
- (5) Tominaga, M.; Suzuki, K.; Kawano, M.; Kusukawa, T.; Ozeki, T.; Sakamoto, S.; Yamaguchi, K.; Fujita, M. *Angew. Chem., Int. Ed.* **2004**, *43*, 5621–5625.
- (6) Related cuboctahedral complexes: (a) Moulton, B.; Lu, J.; Mondal, A.; Zaworotko, M. J. *Chem. Commun.* **2001**, 863–864. (b) Eddaoudi, M.; Kim, J.; Wachter, J. B.; Chae, H. K.; O’Keeffe, M.; Yaghi, O. M. *J. Am. Chem. Soc.* **2001**, *123*, 4368–4369.
- (7) (a) Sonogashira, K.; Tohda, Y.; Hagihara, N. *Tetrahedron Lett.* **1975**, *16*, 4467–4470. (b) Nguetack, J.-F.; Bollitt, V.; Sinou, D. *Tetrahedron Lett.* **1996**, *37*, 5527–5530.
- (8) CSI-MS is quite effective for analyzing the solution structures of metal complexes: (a) Sakamoto, S.; Fujita, M.; Kim, K.; Yamaguchi, K. *Tetrahedron* **2000**, *56*, 955–964. (b) Yamaguchi, K. *J. Mass Spectrom.* **2003**, *38*, 473–490.
- (9) Both **2a** and **2d** showed the same diffusion coefficients ($\log D = -9.62$ in CD₃CN), suggesting that the oligo(ethylene oxide) chains of **2d** are inside the sphere.

JA0540690